(Supplementary Material)

Highly Loaded MXene/Carbon Nanotube Yarn Electrode for Improved Asymmetric Supercapacitor Performance

Jong Woo Park[a1], Dong Yeop Lee[a1], Hyunsoo Kim[a1], Jae Sang Hyeon[a1], Monica Jung de Andrade[a2], Ray H. Baughman[a2] and Seon Jeong Kim[a1,*]

[a1] Center for Self-Powered Actuation, Department of Biomedical Engineering, Hanyang University, Seoul 04763, Korea

[a2] The Alan G. MacDiarmid NanoTech Institute, University of Texas at Dallas, Richardson, TX 75083, USA

* Corresponding author.
Address all correspondence to S. J. Kim at sjk@hanyang.ac.kr

Key words: energy storage, fiber, intercalation

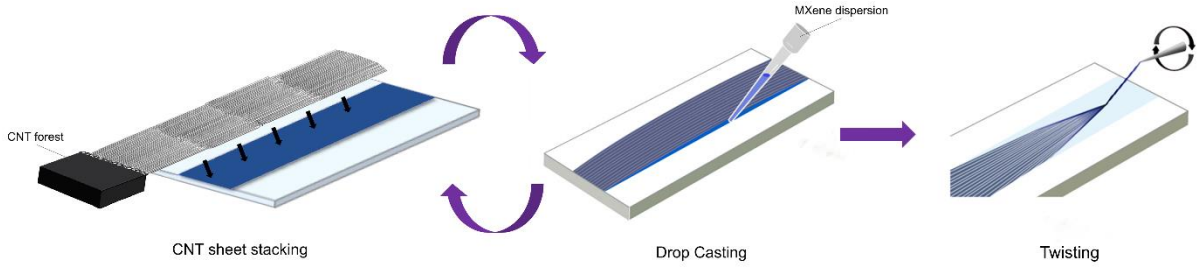

Fig. S1. Schematic illustration of a MXene/CNT biscrolled yarn electrode fabrication. MXene dispersion was drop casted on CNT sheets and dried for a minute and the new layer of CNT sheet was drawn onto the hybrid MXene/CNT film. After repeating the process for few times, the multi-layered MXene/CNT film was scrolled into a yarn by inserting twist.

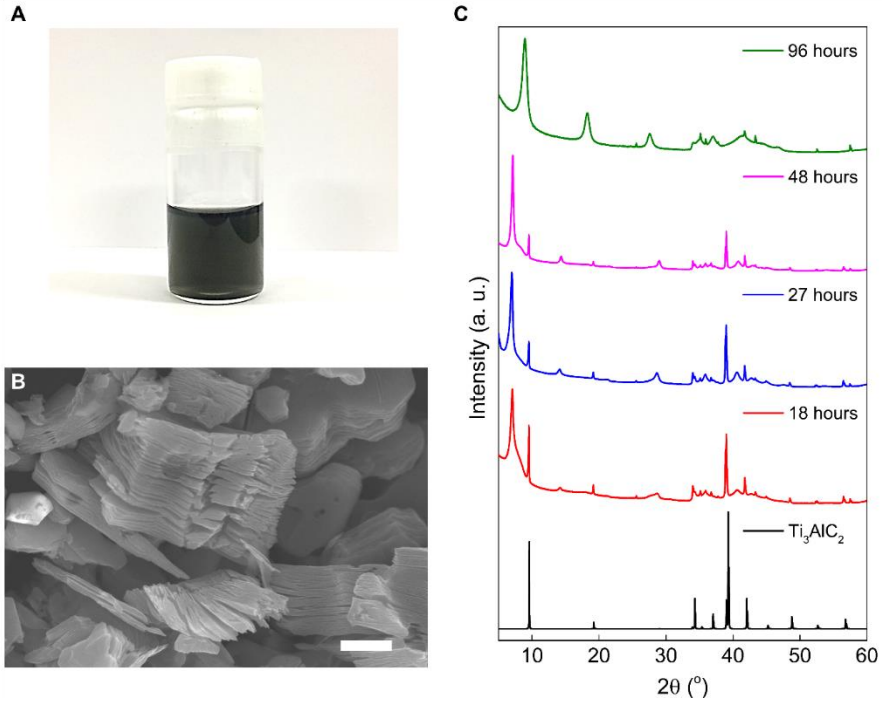

Fig. S2. (A) Optical image of MXene dispersion which is colored as dark green. (~2 mg ml^{-1} in DI water) (B) Scanning electron microscope (SEM) image of 96 hours etched MXene powder. (scale bar = 1.5 μm) (C) X-ray diffractometry (XRD) patterns of the resultant powders of different etching times (18 to 96 hours) and Ti_3AlC_2 raw material. The XRD data from 96 hours etched MXene shows (002) peak shift from 10 to 8.9 degrees.

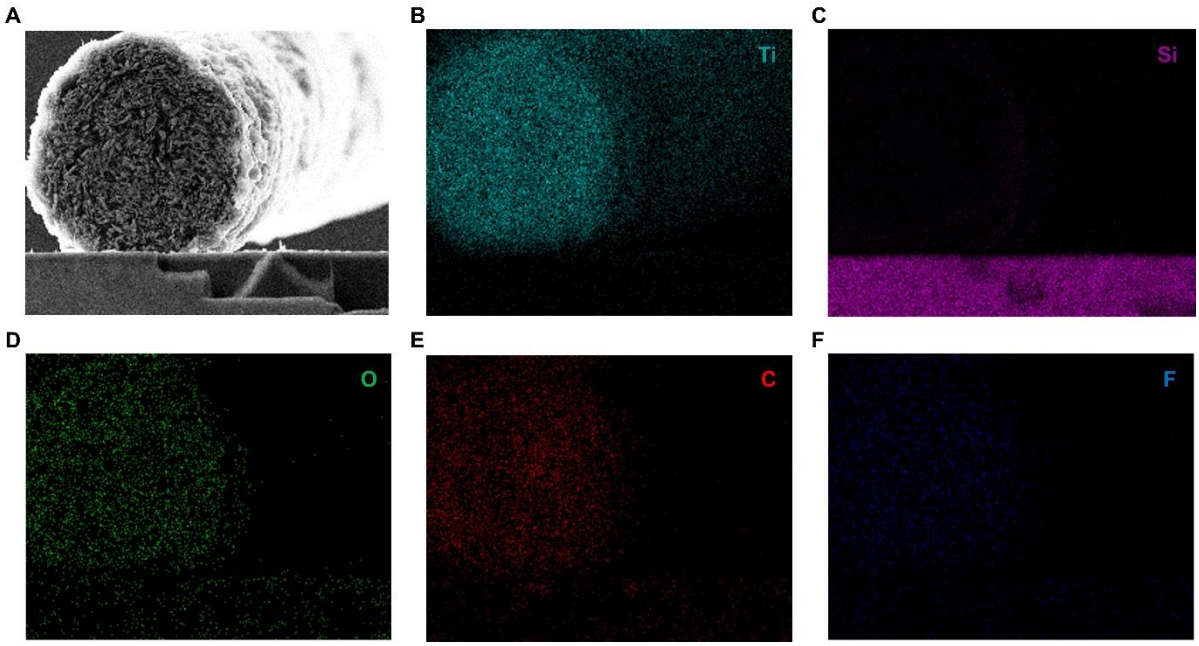

Fig. S3. Energy dispersive spectroscopy (EDS) data of MXene/CNT biscrolled yarn. (A) Cross-sectional SEM image of the biscrolled yarn cut by focused Ga-ion beam. (B, C, D, E, F) Elemental mapping analysis of elements Ti, Si, O, C, F for the cross-sectional image. Ti, O, C, F are well displayed due to the $Ti_3C_2T_x$ MXene (T_x denotes –O and –F) and CNT. Si is for the silicon wafer substrate in the image. The elemental mapping data exhibits that the whole yarn volume is covered with $Ti_3C_2T_x$ (T_x = –OH, –O , or –F) MXene particles.

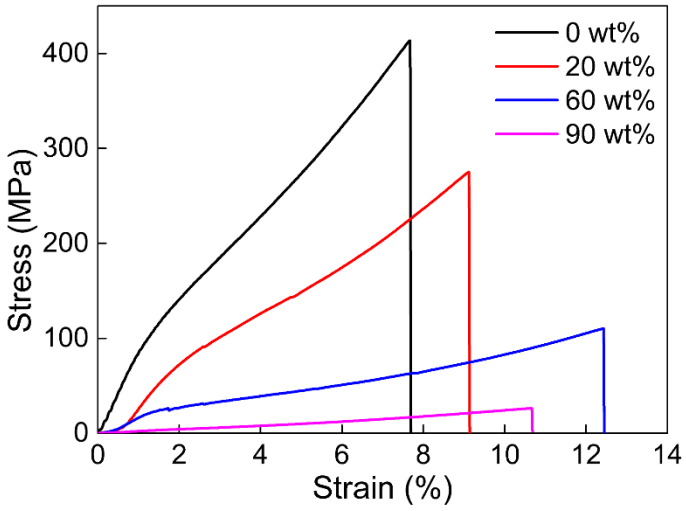

Fig. S4. Strain-stress curve of MXene/CNT biscrolled yarns having different weight ratio of MXene. Toughness of the yarns slightly decreasing until the content of MXene reaches 60 wt% (16.8 MJ m^{-3} to 6.8 MJ m^{-3}) and then dramatically drops (1.3 MJ m^{-3}). Modulus and strength of the yarns are 8.9, 5.5, 2.3, 0.3 GPa, and 414, 275, 110, 26.3 MPa for 0, 20, 60, 90 wt% yarns, respectively.

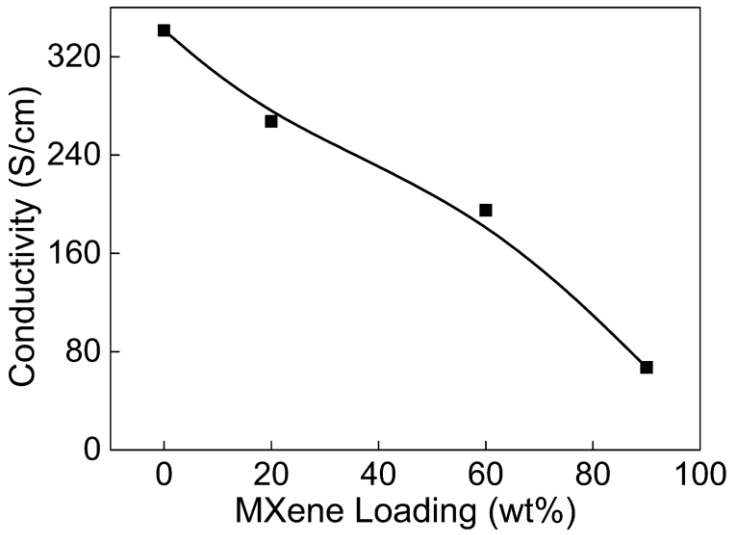

Fig. S5. Conductivity inclination of the biscrolled MXene/CNT yarn by increasing weight fraction of MXene. Since MXene particles have highly conductive nature, the electrical conductivity of the yarn could be retained as 67 S cm^{-1} when the weight ratio of MXene had increased up to 90%.

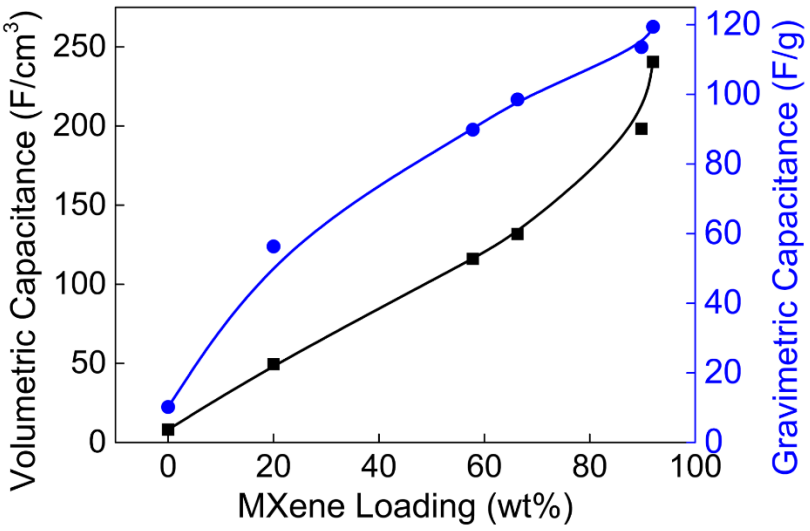

Fig. S6. Volumetric and gravimetric capacitance versus weight ratio of MXene in the biscrolled yarn. The little deviation between two linear plots might be reasoned by the higher volumetric capacitance of MXene than CNT.

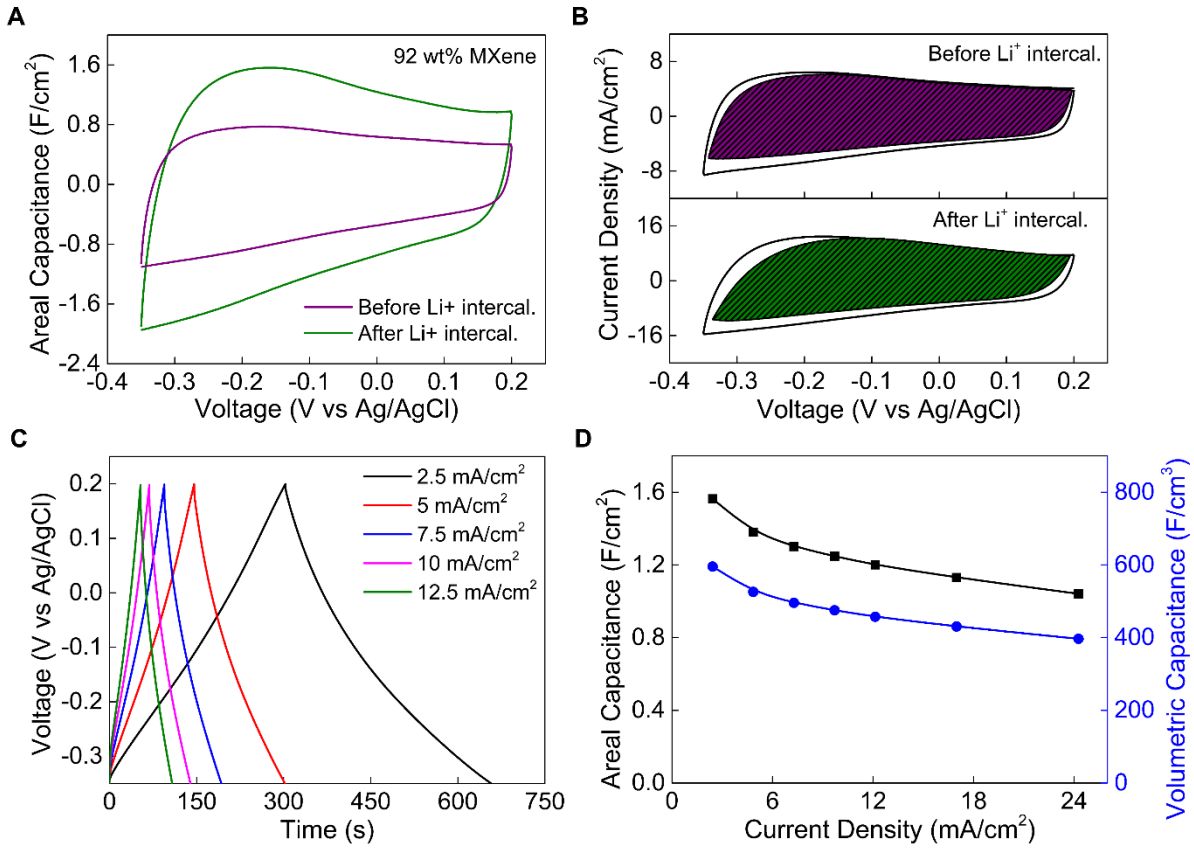

Fig. S7. (A) Cyclic voltammetry (CV) of MXene/CNT yarn in H_2SO_4 electrolyte before and after wetting in LiCl electrolyte. (scan rate = 10 mV s^{-1}) (B) Calculated capacitive contribution of each case, and both graphs have over 82% shaded parts which imply that the mechanism is highly pseudocapacitive. (C) Galvanostatic charge-discharge curve and (D) volumetric and areal capacitance retention as the discharge rate increases (2.5 to 25 mA cm^{-2}) of 93 wt% MXene containing biscrolled yarn after LiCl wetting. The highest areal capacitance 1.56 F cm^{-2} is obtained at 2.5 mA cm^{-2}.

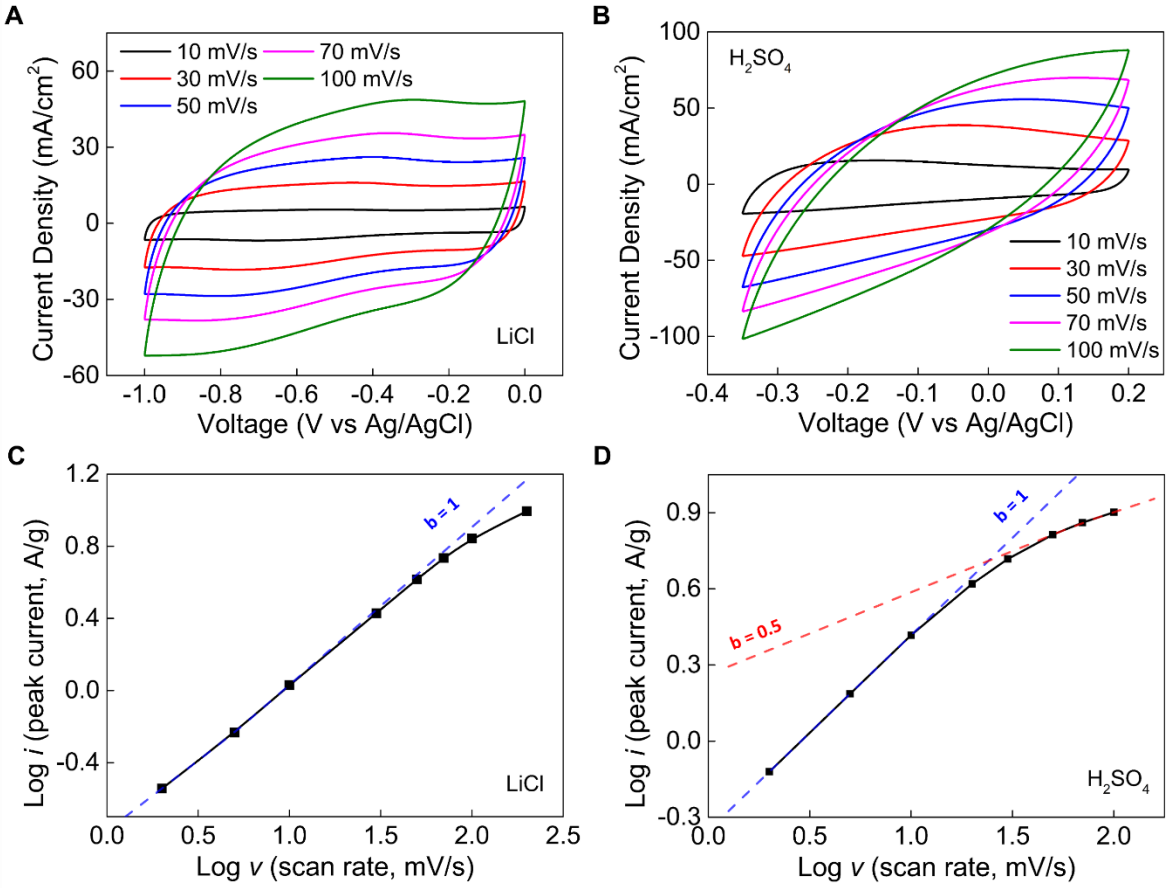

Fig. S8. CV curves of MXene/CNT yarn electrode in (A) 5 M LiCl and (B) 1 M H_2SO_4 electrolytes. (C, D) Logarithmic dependence of anodic peak current i versus scan rate v for different electrolytes. From the power law $i = av^b$, the linear dependence of i on v indicates a capacitive behavior, while the dependence of i on square root of v indicates diffusion limited behavior. (C) In LiCl electrolyte, the MXene/CNT yarn exhibits capacitive behavior for most scan rates, (D) however in H_2SO_4, it exhibits diffusion limited behavior at scan rate over 50 mV s^{-1}.

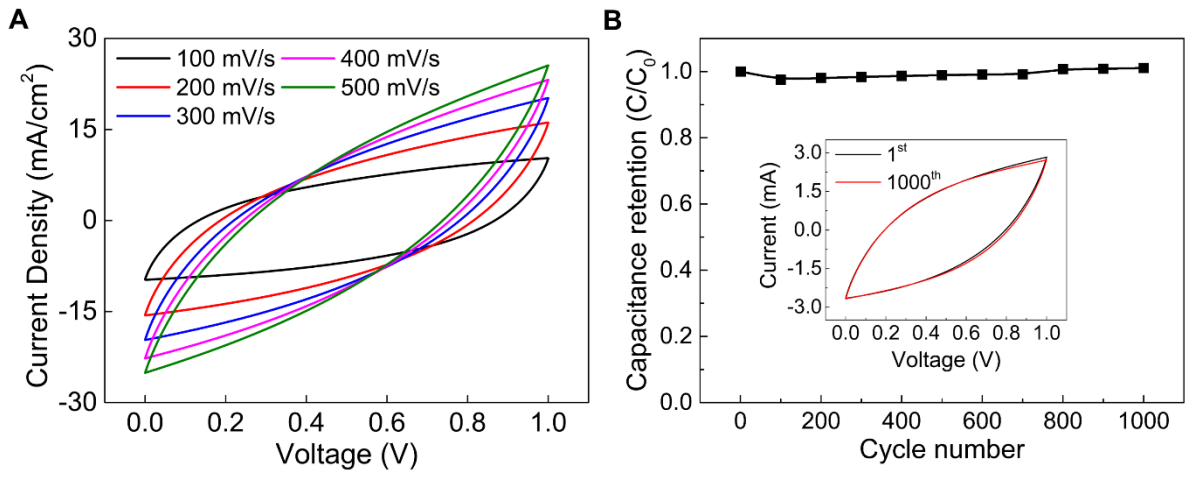

Fig. S9. (A) CV curves of the all-solid-state symmetric MXene/CNT yarn supercapacitor at scan rate 100 to 500 mV s^{-1}. (B) Capacitance retention of the symmetric yarn supercapacitor after 1000 cycles of charging and discharging. Inset shows CV curves before and after 1000 cycles.

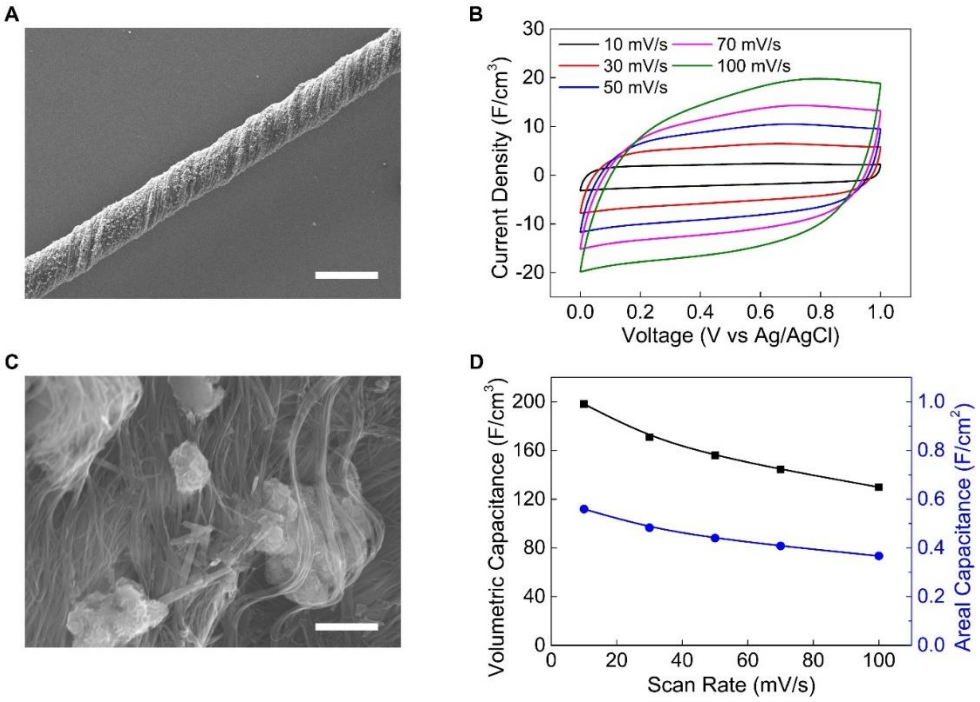

Fig. S10. (A) Scanning electron microscope image of MnO_2/CNT biscrolled yarn and its (C) magnified image which shows the contact between MnO_2 particles and CNT bundles. (B) The CV curve and (D) capacitance retention versus scan rate are plotted. The volumetric and areal capacitance of the MnO_2/CNT biscrolled yarn are 198 F cm^{-3} and 559 mF cm^{-2} at 10 mV s^{-1} respectively, and they are retained 65.6% when scan rate increases to 100 mV s^{-1}.

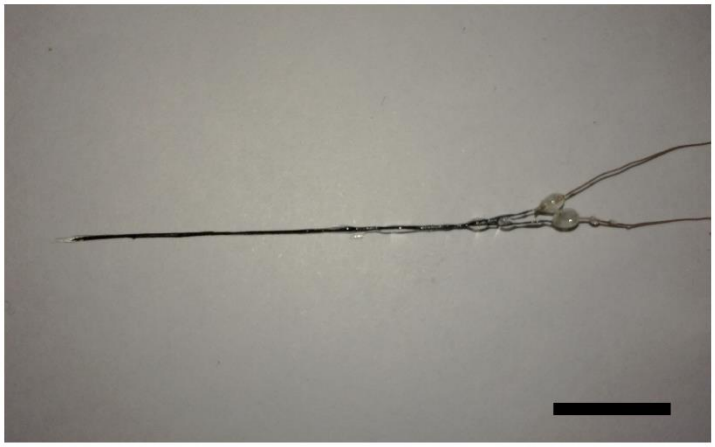

Fig. S11. Optical image of gel-electrolyte coated two-plied asymmetric supercapacitor. The overall diameter is about 350 μm. (scale bar = 1 cm)

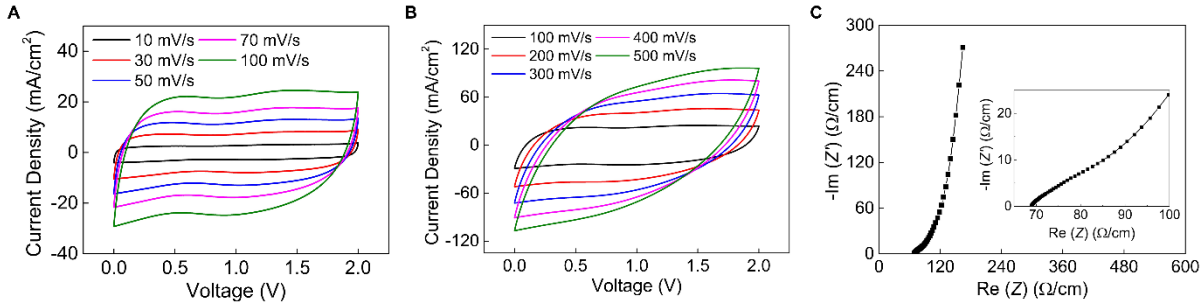

Fig. S12. Cyclic voltammogram of the asymmetric supercapacitor at scan rate (A) 10 to 100 mV s^{-1} and (B) 100 to 500 mV s^{-1}. (C) Nyquist curve of the asymmetric supercapacitor yarn. Magnified inset indicates that the equivalent series resistance is 68 Ω cm^{-1}. The current is normalized by total surface area of the asymmetric supercapacitor including gel electrolyte.

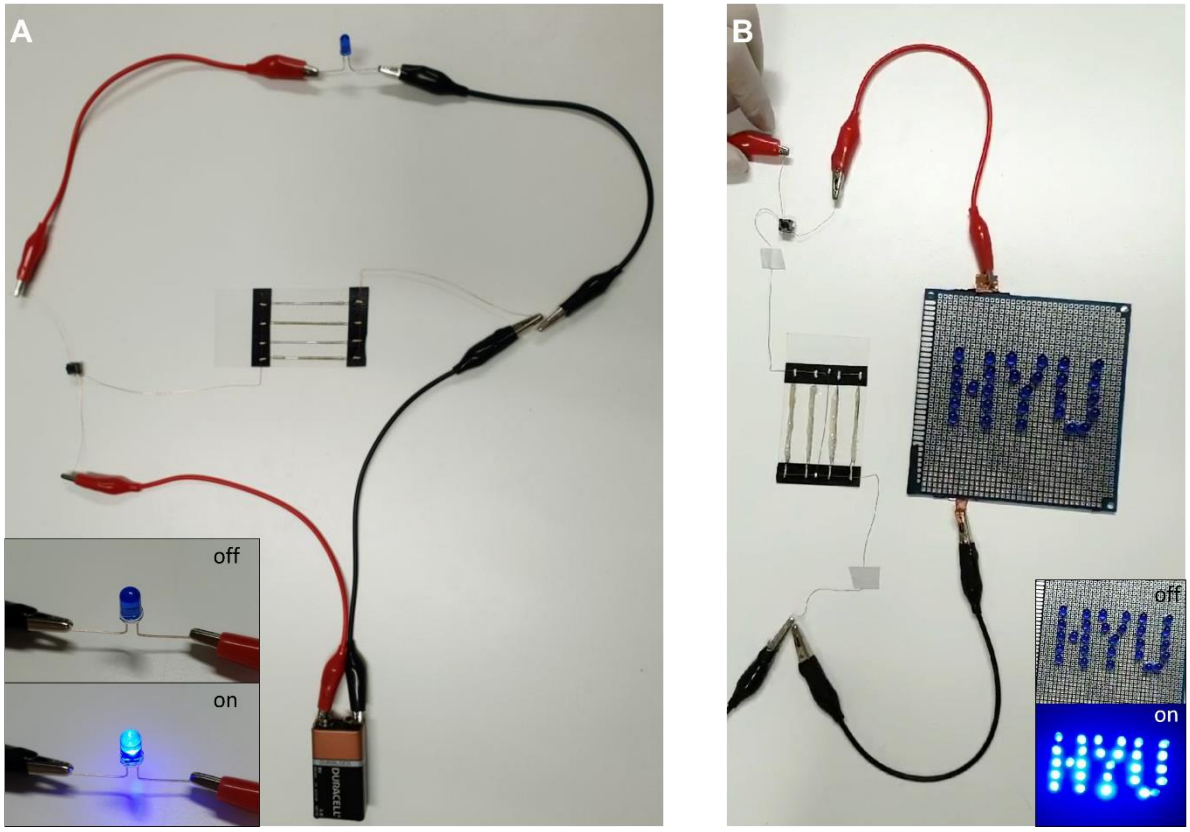

Fig. S13. Optical images of circuits comprising battery, switch, LEDs and set of four supercapacitor cells. Four serial-connected asymmetric yarn supercapacitors was charged by 9 V battery and when the switch is on, the blue LED is lighted by the supercapacitor. (A) The supercapacitor could light up one blue LED for 5 minutes and (B) 28 parallel-connected set of LEDs for about a minute.

Table S1. Comparison of specific capacitances of prior-art yarn type supercapacitor electrodes using MXene.

Electrode	Electrolyte	C_L [mF cm^{-1}]	C_A [mF cm^{-2}]	C_V [F cm^{-3}]	C_m [F g^{-1}]	*Ref*
MXene/CNT biscrolled yarn	1 M H_2SO_4	51.55	1564	595.6	295.7	This work
	PVA/LiCl	68.00*	876.3*	141.9*	93.13*	
MXene/silver plated nylon	PVA/H_2SO_4	50.1	328			22
MXene/PEDOT:PSS on carbon fiber	PVA/H_3PO_4	131.7	658.5	54.7	16.1	23
MXene/rGO wet spun fiber	H_2SO_4		565.4	890.7	494.8	24
MXene/rGO wet spun fiber	H_2SO_4		232.5	340.7	256.7	25

*Capacitances are multiplied by factor four for comparison performance as single electrode.

Table S2. Comparison of specific energies of yarn based asymmetric supercapacitors which are published recently.

Electrode	Electrolyte	Voltage [V]	E_A [µWh cm^{-2}]	E_V [mWh cm^{-3}]	P_A [µW cm^{-2}]	P_V [mW cm^{-3}]	*Ref*
MXene, MnO_2/CNT plied yarn	PVA/LiCl	2	100	8.17	260	21.2	This work
VN/C, MnO_2/PEDOT:PSS/CNT coaxial fiber	PVA/Na_2SO_4	1.8	96.07		270		9
VN, Zn-Ni-CoO_3/CNT twisted fiber	PVA/KOH	1.6	53.33	17.78	240	80	10
PEDOT/MnO_2, C/Fe_3O_4 on steel fibers	PVA/LiCl	2	33.5	4.02	600	72	8
Ni-$NiCo_2S_4$, N-rGO coated nickel wires	PVA/KOH	1.4	32.67	5.33	356.8	57.04	5
$ZnCo_2O_4$/Zn-Co-S, H-Co_3O_4/CoNC at CNT fibers	PVA/KOH	1.4	32.01		698.4		13
MnO_2, rGO/CNT yarn	PVA/LiCl	2.1	30.1	3.8	256.7	256.7	6
MnO_2, PPy/CNT coaxial fiber	PVA/KOH	1.5	13.51	2.11	1620	253.56	7
Ni-Co DH/nickel, nickel on carbon fibers	PVA/KOH	1.6	9.57		492.17		4
Co_3O_4/MnO_2 on Ni wire, carbon fiber with graphene	PVA/KOH	1.5	4.34		75		12